ARTICLE

Electron Momentum Spectroscopy of Ethanethiol Complete Valence Shell

Xin-xia Xue, Mi Yan, Fang Wu, Xu Shan, Ke-zun Xu, Xiang-jun Chen*

Hefei National Laboratory for Physical Sciences at Microscale and Department of Modern Physics, University of Science and Technology of China, Hefei 230026, China

(Dated: Received on May 18, 2008; Accepted on June 5, 2008)

The binding energy spectra and electron momentum distributions for the complete valence orbitals of ethanethiol were measured for the first time by binary (e, 2e) electron momentum spectroscopy employing non-coplanar symmetric kinematics at an impact energy of 1200 eV plus binding energy. The experimental results are generally consistent with the theoretical calculations using density functional theory and Hartree-Fock methods with various basis sets. A possible satellite line at 17.8 eV in binding energy spectrum was observed and studied by electron momentum spectroscopy.

Key words: Ethanethiol, Electron momentum spectroscopy, Valence orbital, Satellite line, Binding energy spectrum

I. INTRODUCTION

Electron momentum spectroscopy (EMS) has been used extensively for investigations of electronic structures of atoms, molecules and condensed matter in the last three decades [1-3]. Basically two types of information can be obtained by EMS: binding energy spectra (BES) over a wide energy range usually covering the complete valence shell, and angular distributions of (e, 2e) cross section for individual transitions giving rise to the peaks in BES. Within the plane wave impulse approximation (PWIA) and the target Hartree-Fock (THFA) [1] or target Kohn-Sham approximation (TKSA) [4], this measured (e, 2e) cross section is proportional to the spherically averaged momentum distribution of a specific molecular orbital (MO).

Ethanethiol (C_2H_5SH) has been used for many years in the gas industry as warning agents to protect against explosions, fires, and other hazards by giving a distinctive odor. As a fundamental mercaptan, ethanethiol has been the subject of several experimental studies including He I photoelectron spectroscopy (PES) [5,6], microwave spectra [7-9], far-infrared spectra [10], and Raman spectra [11].

The only previous EMS study on ethanethiol has been reported by Takahashi *et al.* together with several other molecules [12]. In their work, the authors concentrated on revealing the delocalization characteristics of the highest occupied sulfur lone pair orbitals by comparing the experimental momentum profiles (XMP) with the calculated momentum profile for atomic sulfur 3p orbital.

In this work, EMS study on the complete valence shell of ethanethiol is reported for the first time. Individual experimental momentum distributions for all valence orbitals have been obtained and the results are compared with theoretical calculations by using Hartree-Fock and density functional theory (DFT) methods with various basis sets up to aug-cc-pVDZ.

II. EXPERIMENTAL AND THEORETICAL BACKGROUND

EMS is based on the high-energy electron impact single ionization process. An incident electron with energy E_0 causes the target molecule to be ionized. By detecting the two outgoing (scattered and ionized) electrons in coincidence, the kinematics of the reaction can be completely determined. Under symmetric non-coplanar geometry, in which the two outgoing electrons are selected to have equal energies (E_1=E_2), equal polar angles (θ=θ_1=θ_2=45°) and a varying relative azimuthal angle ϕ, the magnitude of the target electron momentum is given by

$$p = \left[(2p_1 \cos\theta - p_0)^2 + \left(2p_1 \sin\theta \sin\frac{\phi}{2} \right)^2 \right]^{1/2} \quad (1)$$

where p_0 is the momentum of the incident electron and p_1 is the momentum of the outgoing electrons. Within several approximations, including the binary encounter approximation, the plane wave impulse approximation (PWIA), and the target Hartree-Fock approximation (THFA), the triple differential cross-section for randomly oriented molecule is given by [1-3]

$$\sigma_{\mathrm{EMS}} \propto S_i^{(\mathrm{f})} \int \mathrm{d}\Omega_p \, |\varphi_i(\vec{p})\rangle^2 \quad (2)$$

where $|\varphi_i(\vec{p})\rangle$ is the one-electron canonical HF wave function in momentum space for the ith orbital from which the electron is ionized. $S_i^{(\mathrm{f})}$ is the spectroscopic factor (also known as the pole strength), which is the

*Author to whom correspondence should be addressed. E-mail: xjun@ustc.edu.cn, FAX: +86-551-3606266

probability of producing a one-hole configuration in the final ion state f. Estimates of $S_i^{(\mathrm{f})}$ values for a certain transition can be obtained from a comparison of the relevant calculated and experimental cross sections. The wave function $|\varphi_i(\vec{p})\rangle$ is the Fourier transform of the more familiar one-electron position space orbital wave function $|\varphi_i(\vec{r})\rangle$.

The triple differential cross-section has been reinterpreted [4] more recently within target Kohn-Sham approximation (TKSA) by simply replacing the canonical Hartree-Fock orbital in Eq.(2) with the momentum space Kohn-Sham orbital $\varphi^{\mathrm{KS}}(\vec{p})$. We then have

$$\sigma_{\mathrm{EMS}} \propto S_i^{(\mathrm{f})} \int \mathrm{d}\Omega_p |\varphi_i^{\mathrm{KS}}(\vec{p})\rangle^2 \tag{3}$$

The integrals in Eqs.(2) and (3) are known as the spherically averaged one-electron momentum distributions, i.e. electron momentum profiles. The theoretical momentum profiles (TMPs) for the valence orbitals of ethanethiol were calculated using THFA and TKSA. The corresponding position space canonical HF^- or KS-DFT orbital wave functions were calculated employing 6-31G, 6-311G, 6-311++G**, cc-pVDZ, and aug-cc-pVDZ basis sets using GAUSSIAN 98W [13]. The Fourier transform was subsequently applied to obtain the momentum space wavefunctions. The DFT calculations were performed using the B3LYP hybrid functional. The geometry of ethanethiol was adopted from microwave spectroscopy [9] and optimized by B3LYP/6-311++G**.

The details of the spectrometer have been given elsewhere [14]. Briefly, it consists of an electron gun, a reaction chamber, two hemispherical electron energy analyzers each having a five-element cylindrical retarding lens and a one-dimensional position sensitive detector. One analyzer is kept fixed while the other one can be rotated over an azimuthal angle range from –30° to 30°. An incident electron energy of 1.2 keV plus binding energy was employed and the coincident energy resolution and the momentum resolution of the spectrometer were determined to be 1.3 eV (in full width at half maximum) and 0.15 a.u. by measuring argon 3p ionization. The gas sample of C_2H_5SH with 97.0% purity was used without further purification. No impurities were evident in the binding energy spectra.

III. RESULTS AND DISCUSSIONS

C_2H_5SH coexists in two conformers: gauche and trans. The population ratio of the trans and gauche conformers at room temperature was determined to be 1:4 [12].

The gauche conformer has C_1 symmetry point group, and its ground state electronic configuration can be written as

$$(\mathrm{core})^{14} \underbrace{(8\mathrm{a})^2(9\mathrm{a})^2(10\mathrm{a})^2}_{\text{Inner valence shell}} \underbrace{(11\mathrm{a})^2(12\mathrm{a})^2(13\mathrm{a})^2(14\mathrm{a})^2(15\mathrm{a})^2(16\mathrm{a})^2(17\mathrm{a})^2}_{\text{Outer valence shell}}$$

while the trans conformer has C_s symmetry point group, and its ground state electronic configuration can be written as

$$(\mathrm{core})^{14} \underbrace{(7\mathrm{a}')^2(8\mathrm{a}')^2(9\mathrm{a}')^2}_{\text{Inner valence shell}} \underbrace{(2\mathrm{a}'')^2(10\mathrm{a}')^2(11\mathrm{a}')^2(12\mathrm{a}')^2(3\mathrm{a}'')^2(13\mathrm{a}')^2(4\mathrm{a}'')^2}_{\text{Outer valence shell}}$$

A. Binding energy spectra

Sixteen binding energy spectra over the energy range of 7-30 eV which covers seven outer valence orbitals and three inner valence orbitals were collected at the out-of-plane azimuth angles 0°, 1°, 2°, 3°, 4°, 5°, 6°, 7°, 8°, 9°, 11°, 13°, 15°, 17°, 21°, and 24° in a series of sequential repetitive scans. Data for 0°, 7°, and the sum of all ϕ are shown in Fig.1. The BES are fitted with a set of individual Gaussian peaks corresponding to the ionizations from individual MOs numbered 8-17 as indicated by dashed lines, while the overall fitted spectra are represented by the solid lines. The widths of the peaks are the combinations of the present EMS instrumental energy resolution and the corresponding Franck-Condon widths derived from the high resolution PES [5]. The positions of the peaks for outer valence orbitals are also determined by high resolution PES [5] with tiny adjustments to compensate for the asymmetry of the Franck-Condon profiles. The BES for inner valence orbitals in the energy range from 19 eV to 29 eV are obtained for the first time. The ionization potentials are determined to be 20.6, 22.9, and 25.6 eV by fitting Gaussian peaks to the experimental data. A satellite structure at 18.0 eV was identified by PES work [6]. In order to best fit the present experimental BES, a Gaussian peak at about the same position should also be included and indicated by 's' as shown in Fig.1.

The experimental ionization potentials obtained by PES measurements [5,6] and present EMS work, together with the calculated results by outer valence Green's function (OVGF) methods for two conformers of ethanethiol, are listed in Table I. As can be seen, the ionization potentials for the two conformers have nearly the same values for each corresponding MO and therefore contribute to the same ionization peaks in BES. The pole strengths for outer valence orbitals are also obtained by OVGF and listed in brackets in Table I.

DOI:10.1088/1674-0068/21/06/515-520

TABLE I Ionization potentials for valence orbitals of ethanethiol (pole strengths are listed in brackets).

Orbitals			Ionization potentials/eV				
MO	Gauche	Trans	PES [5]	PES [6]	EMS	Gauche[a]	Trans[a]
17	17a	4a″	9.29	9.36	9.3	8.86 (0.92)	8.84 (0.92)
16	16a	13a′	11.59	11.65	11.6	11.33 (0.91)	11.4 (0.91)
15	15a	3a″	12.61	12.59	12.5	12.61 (0.91)	12.7 (0.91)
14	14a	12a′		13.38	13.3	13.22 (0.91)	12.96 (0.91)
13	13a	11a′		14.17	14.1	13.94 (0.90)	13.61 (0.90)
12	12a	10a′		15.28	15.4	14.89 (0.90)	15.49 (0.90)
11	11a	2a″		16.06	16.4 (0.90)	15.91 (0.90)	15.75 (0.90)
s				∼18.00	17.8		
10	10a	9a′			20.6		
9	9a	8a′			22.9 (0.60)		
8	8a	7a′			25.6 (0.50)		

[a] Calculated resulted by OVGF/6-311++G**.

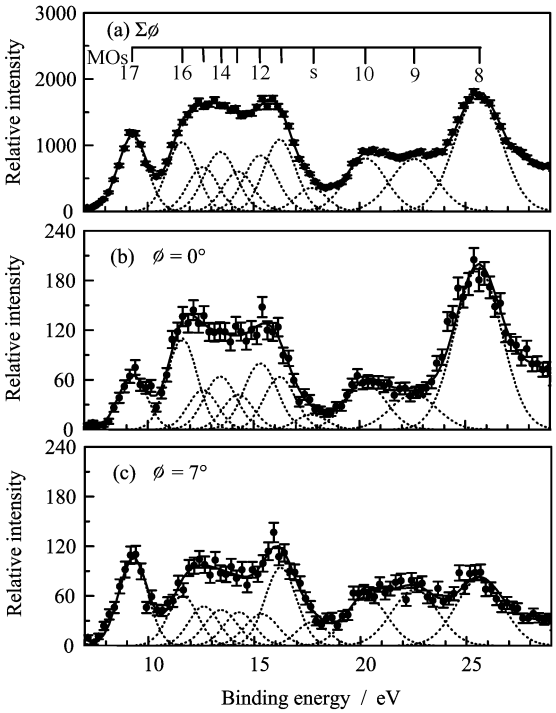

FIG. 1 Binding energy spectra for ethanethiol at (a) the sum of all angles, (b) ϕ=0°, and (c) ϕ=7°. The dashed lines represent Gaussian fits to the peaks and the solid curve is the summed fit.

B. Experimental and calculated momentum distributions

The XMPs are extracted by deconvoluting the same peak from the sequentially obtained binding energy spectra at different ϕ and plotting area under the corresponding fitted peaks as a function of momentum p (i.e. ϕ). Since ethanethiol coexists in two conformers, the Boltzmann-weighted abundances should be taken into account when comparing the XMPs with theoretical calculations. The population ratio of the trans and gauche conformers at room temperature has been determined to be 1:4 [12], thus all the TMPs in the following discussions are the summation of the respective TMPs, 20% for the trans and 80% for the gauche conformers. Furthermore, the XMPs and TMPs are placed on a common intensity scale by normalizing the XMPs for HOMO (MO17, well resolved in BES) of ethanethiol and all the TMPs have been convoluted by the instrumental momentum resolution of 0.15 a.u. by utilizing the Gaussian-weighted planar grid method (GWPG) [15].

Although 11 Gaussian peaks corresponding to the ionizations from all the individual valence orbitals are fitted to the BES (including one peak for satellite structure at 17.8 eV), some of the bands can not be well resolved due to the small energy spacing and the low energy resolution of the spectrometer. In such a case, the individual momentum profiles are scattered and not reliable. Therefore, only the summed momentum profiles will be presented in this work.

In Fig.2(a), we compare the XMP for HOMO (MO17), corresponding to the ionization band at 9.3 eV in BES, with the TMPs. It is immediately apparent from Fig.2(a) that the XMP for this orbital is "p-type" in nature, confirming the previous EMS conclusion [12] that this orbital is characterized as a sulfur lone pair orbital. The level of agreement, within the experimental uncertainties on the data, between XMP and TMPs is fair. All the calculated momentum profiles reproduce the shape of XMP. Except for the low quality basis set of 6-31G and basis set of cc-pVDZ with no diffuse function added, all the calculations describe the experiment well. It can be expected that TMP calculated with B3LYP/cc-pVDZ predict a momentum profile shifted to the larger momentum region. Since the high momentum region roughly corresponds to the area close

DOI:10.1088/1674-0068/21/06/515-520

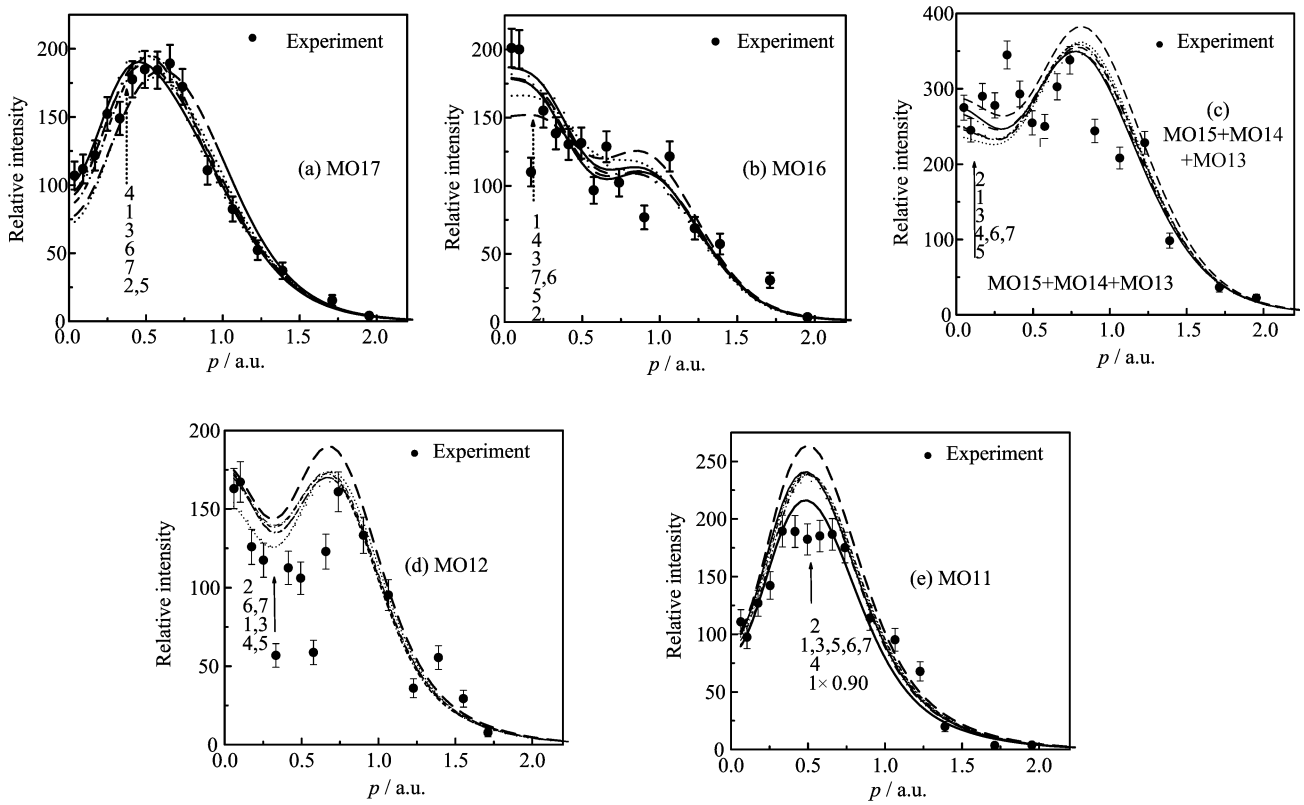

FIG. 2 Experimental and theoretical momentum profiles for HOMO of ethanethiol. 1: B3LYP/aug-cc-pVDZ, 2: B3LYP/cc-pVDZ, 3: B3LPY/6-311++G**, 4: B3LYP/6-311G, 5: B3LYP/6-31G, 6: HF/aug-cc-pVDZ, and 7: HF/6-311++G**.

to nuclei in coordinate space, therefore without a diffuse function added, the cc-pVDZ basis set will predict a more compacted electron distribution in coordinate space and hence a more expanded momentum distribution, as is the case for this orbital.

As for the next orbital (MO16) with binding energy of 11.6 eV, it is dominantly characterized by a C–S σ orbital and the XMP exhibit mainly "s-type" (maximum density at p=0) mixed with "p-type" (a secondary maximum with lower intensity at about p=0.9 a.u.) profile as shown in Fig.2(b). Among all the calculated momentum profiles, B3LYP/aug-cc-pVDZ best describes the XMP, not only predicting the positions of maximum but also the intensity of the profile. All the other calculations underestimate the intensity in the low momentum region. The calculation with cc-pVDZ basis set again fails to reproduce the experiment, predicting a lower intensity in the low momentum region and a higher intensity in the second maximum region.

As we have mentioned, the next three orbitals (MO15 to MO13) have close values of ionization potentials and are beyond the resolving ability of the present instrument. Therefore, only the summed XMP are presented in Fig.2(c). All the calculations roughly reproduce the experiment, except three points, one at p=0.33 a.u. where the experimental data has much higher intensity, and two at p=0.90 and 1.06 a.u. where measurements have obvious lower intensity. The deviations may due to the deconvolution procedure. We only include the statistical errors for experiment data in this article; if the deconvolution errors are considered, this deviation is not surprising for these small energy spacing ionization bands.

Figure 2(d) shows the XMP for MO12 at 15.4 eV in BES. Although the small energy spacing of this ionization band from the adjacent ones makes the data rather scattered, the XMP exhibit an "sp-type" character with two maxima of electron density at p=0 and $p\approx$0.7 a.u. as theoretical calculations predicted. However, the large deconvolution errors make the evaluation of theoretical calculations rather difficult. Among all the TMPs, the one calculated by B3LYP/cc-pVDZ mostly severely overestimates the experiment.

The XMP for MO11 at binding energy of 16.4 eV is shown in Fig.2(e). The experimental intensity is somewhat weaker in strength than what is expected in the relevant calculated momentum profiles, thus indicating that there must be further intensity of the ionization from this orbital to be found elsewhere in the binding energy spectra. The agreement between XMP and TMPs becomes better when the calculated results are scaled by a factor of 0.90 (shown as solid curve labeled with 1×0.90), representing the spectroscopic factor for the ionization state at binding energy of 16.4 eV.

DOI:10.1088/1674-0068/21/06/515-520

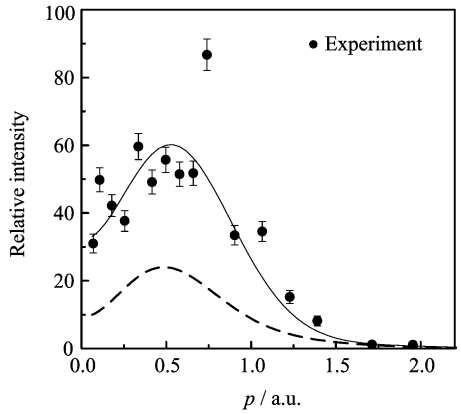

FIG. 3 Experimental momentum profile for the satellite structure at 17.8 eV (solid circles). The dashed curve is the theoretical momentum profile for MO11 scaled by a factor of 0.10. The solid curve is the summation of 10% of theoretical momentum profile for MO11 and 15% of that for MO10.

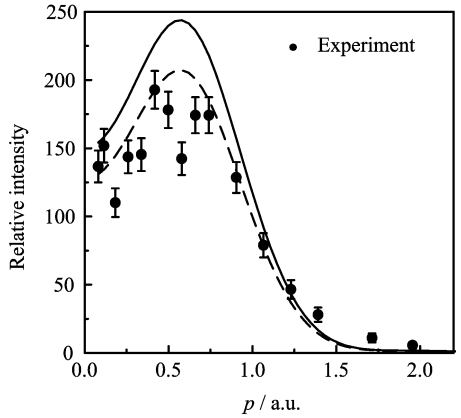

FIG. 4 Experimental momentum profile for MO10 of ethanethiol (solid circles). The solid curve is the theoretical momentum profile while the dashed curve is scaled by a factor of 0.85.

As we mentioned above, a satellite structure at 18.0 eV was identified by PES work [6]. In order to best fit the present experimental BES, a Gaussian peak at 17.8 eV should also be included. The XMP for this band is shown in Fig.3. The missing pole strength for the ionization of MO11 is most likely to be found in this satellite structure. However, some 10% intensity of TMP (calculated by B3LYP/aug-cc-pVDZ) for MO11 (shown as dashed curve in Fig.3) is not enough to describe the experiment, not only in shape but also in intensity. We noticed in BES that it is possible for this ionization band to be contaminated by the adjacent ionization band for MO10 whose Franck-Condon profile width is considerably large. The XMP for MO10 is presented in Fig.4. This is the outermost inner valence orbital of ethanethiol. It can immediately be inferred from Fig.4 that the XMP is somewhat weaker in

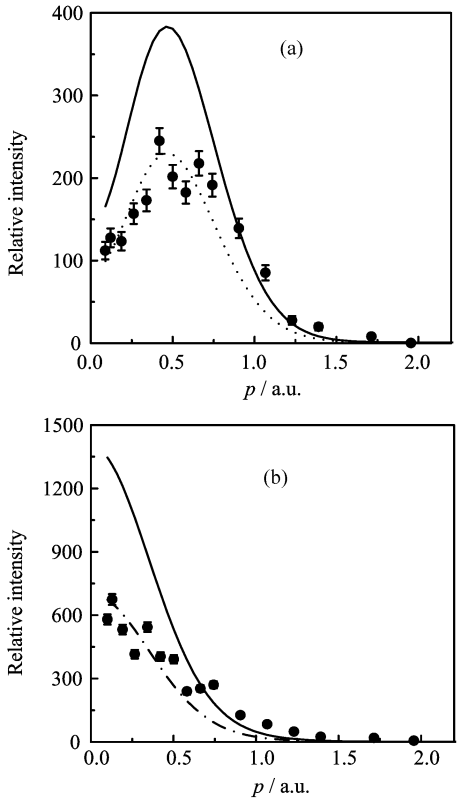

FIG. 5 Experimental momentum profile for MO9 (a) and MO8 (b) of ethanethiol (solid circles). The solid curve is the theoretical momentum profile while the dashed curve is scaled by a factor of 0.60 (a) and 0.50 (b).

strength than the TMP (calculated by B3LYP/aug-cc-pVDZ). The fair agreement can be approached when the TMP is scaled by a factor of 0.85, indicating that some 15% intensity is missing. The missing intensity can be found in the XMP for the aforementioned satellite structure probably due to the deconvoluting contamination. By adding 15% of TMP for MO10 (solid curve in Fig.3), a fair agreement can be obtained.

The XMPs for the two innermost ionization bands located at 22.9 and 25.6 eV, corresponding to the two inner valence orbitals MO9 and MO8, are shown in Fig.5. The XMP for MO9 is "p-type" in nature, while the XMP for MO8 is "s-type". It is apparent from Fig.5 that both XMPs are much weaker in strength than the TMPs (calculated by B3LYP/aug-cc-pVDZ), indicating the significant final state correlation effects. An agreement between the XMPs and the TMPs can be achieved when the calculated results are multiplied by factors of 0.60 and 0.50 (shown as dashed curves) respectively, representing the experimental spectroscopic factors for the ionization states at binding energies of 22.9 and 25.6 eV. Significant intensity can be observed in the energy range larger than 27 eV in BES, which could be contributed to the missing pole strengths for ionizations from the two innermost valence orbitals.

DOI:10.1088/1674-0068/21/06/515-520

IV. CONCLUSION

The binding energy spectra and electron momentum distributions for the complete valence orbitals of ethanethiol (C_2H_5SH) were studied by binary (e, 2e) electron momentum spectroscopy employing noncoplanar symmetric kinematics at impact energy of 1.2 keV plus binding energy. The binding energy spectra for inner valence orbitals in the energy range from 19 eV to 29 eV are obtained for the first time. The ionization potentials are determined to be 20.6, 22.9, and 25.6 eV by fitting Gaussian peaks to the experimental data. The experimental momentum profiles for the valence orbitals of ethanethiol are compared with the theoretical momentum profiles calculated using HF and B3LYP method with 6-31G, 6-311G, 6-311++G**, cc-pVDZ, and aug-cc-pVDZ basis sets. Basically, B3LYP/aug-cc-pVDZ best reproduced the experiments, while the calculations employing cc-pVDZ basis sets with no diffuse functions failed to describe the measured results. Significant final state correlation effects were observed and the spectroscopic factors for the ionization transitions for the two innermost valence orbitals are experimentally determined. A satellite structure at 17.8 eV in BES was confirmed by comparison of the experimental momentum profile with the theoretical calculations.

V. ACKNOWLEDGMENTS

This work was supported by the National Natural Science Foundation of China (No.10734040) and the Foundation for Major Research Program of Education Department of Anhui Province (No.ZD2007002-1).

[1] I. E. McCarthy and E. Weigold, Rep. Prog. Phys. **54**, 789 (1991).
[2] M. A. Coplan, J. H. Moore, and J. P. Doering, Rev. Mod. Phys. **66**, 985 (1994).
[3] E. Weigold and I. E. McCarthy, *Electron Momentum Spectroscopy*, New York: Kulwer, (1999).
[4] P. Duffy, D. P. Chong, M. E. Casida, and D. R. Salahub, Phys. Rev. A **50**, 4704 (1994).
[5] H. Ogata, H. Onizuka, Y. Nihei, and H. Kamada, Bull. Chem. Soc. Jpn. **46**, 3036 (1973).
[6] K. Kimura, S. Katsumata, Y. Achiba, T. Yamazaki, and S. Iwata, *Handbook of He I Photoelectron Spectra of Fundamental Organic Molecules*, New York: HALSTED, (1981).
[7] J. Nakagawa, K. Kuwada, and M. Hayashi, Bull. Chem. Soc. Jpn. **49**, 3420 (1976).
[8] M. Hayashi, M. Imaishi, and K. Kuwada, Bull. Chem. Soc. Jpn. **47**, 2382 (1974).
[9] R. E. Schmidt and C. R. Quade, J. Chem. Phys. **62**, 3864 (1975).
[10] A. S. Manocha, W. G. Fateley, and T. Shimanouchi, J. Phys. Chem. **77**, 1977 (1993).
[11] J. R. Durlg, W. E. Bucy, and C. J. Wurrey, J. Phys. Chem. **79**, 988 (1995).
[12] M. Takahashi, H. Nagasaka, and Y. Udagawa, J. Phys. Chem. A **101**, 528 (1997).
[13] M. J. Frisch, G. W. Trucks, H. B. Schlegel, G. E. Scuseria, M. A. Robb, J. R. Cheeseman, V. G. Zakrzewski, J. J. A. Montgomery, R. E. Stratmann, J. C. Burant, S. Dapprich, J. M. Millam, A. D. Daniels, K. N. Kudin, M. C. Strain, O. Farkas, J. Tomasi, V. Barone, M. Cossi, R. Cammi, B. Mennucci, C. Pomelli, C. Adamo, S. Clifford, J. Oehterski, G. A. Petersson, P. Y. Ayala, Q. Cui, K. Morokuma, D. K. Malick, A. D. Rabuck, K. Raghavachari, J. B. Foresman, J. Cioslowski, J. V. Ortiz, B. B. Stefanov, G. Liu, A. Liashenko, P. Piskorz, I. Komaromi, R. Gomperts, R. L. Martin, D. J. Fox, T. Keith, M. A. Al-Laham, C. Y. Peng, A. Nanayakkara, C. Gonzalez, M. Challacombe, P. M. W. Gill, B. Johnson, W. Chen, M. W. Wong, J. L. Andres, C. Gonzalez, M. Head-Gordon, E. S. Replogle, and J. A. Pople, *Gaussian 98, Revision A3*, Pittsburgh: Gaussian, Inc. (1998).
[14] B. X. Yang, X. J. Chen, W. N. Pang, M. H. Chen, F. Zhang, B. L. Tian, and K. Z. Xu, Acta Phys. Sin. **5**, 862 (1997).
[15] P. Duffy, M. E. Casida, C. E. Brion, and D. P. Chong, Chem. Phys. **159**, 347 (1992).

DOI:10.1088/1674-0068/21/06/515-520